SIMULTANEOUS STRUCTURE AND TEXTURE COMPACT REPRESENTATIONS

[1,2] *Jean-François Aujol,* [2]*Basarab Matei*

[1]aujol@math.unice.fr
[1]Laboratoire J.A.Dieudonné , UMR CNRS 6621, Université de Nice Sophia-Antipolis
Parc Valrose, 06108 Nice Cedex 2 , France
[2]ARIANA, projet commun CNRS/INRIA/UNSA, INRIA Sophia Antipolis
2004, route des Lucioles, BP93, 06902, Sophia Antipolis Cedex, France
[3]matei@ann.jussieu.fr
[3]Laboratoire J.L. Lions , UMR CNRS 7598, Université Paris VI
Boîte courrier 187, 4 place Jussieu, 75013 Paris, France

ABSTRACT

In this paper, we tackle the problem of image nonlinear approximation. During the last past years, many algorithms have been proposed to take advantage of the geometry of the image. We intend here to propose a new nonlinear approximation algorithm which would take into account the structures of the image, and which would be powerful even when the original image has some textured areas. To this end, we first split our image into two components, a first one containing the structures of the image, and a second one the oscillating patterns. We then perform the nonlinear approximation of each component separately. Our final approximated image is the sum of these two approximated components. This new nonlinear approximation algorithm outperforms the standard biorthogonal wavelets approximation.

1. INTRODUCTION

Image nonlinear approximation is a very active field of research. The aim is to find a sparse representation for an image, so that one needs to store few coefficients to retrieve the image.
Wavelets have proved to be a powerful tool in this area [1]. They indeed provide sparse representations for images (especially for texture images). But (see [1] for instance), edges lead to many significant wavelet coefficients. That is why there have been a lot of works these last past years to find sparse representations of images that would better take into account the geometry of the images. Some algorithms [2, 3, 4, 5, 6, 7, 8, 9] have thus been proposed to improve wavelets approximation by taking advantage of the structures in the image. Such methods have proved to be efficient for geometrical images.
We want to propose a framework which would extend these methods to images containing both structure and texture information. Structure approximation and texture approximation are not done with the same algorithms. Therefore, we first want to split the image, that we want to approximate, into a geometrical part and a texture part, and then to carry out the approximation of both components separately. To achieve our goal, we are going to use a decomposition algorithm recently introduced in [10, 11, 12]. Such an approach has been successfully introduced in [13] for image inpainting.

The plan of the paper is as follows. We first present the decomposition model of [11, 12]: we recall its link with Meyer's model [14], and show some numerical examples. We then introduce the nonlinear approximation algorithm of [5]: it is well adapted for geometrical images. And we use the classical 7-9 biorthogonal wavelets [1] for textured images. This way, we are in position to describe our new nonlinear approximation algorithm. We show some numerical results to illustrate the relevance of our method. We end the paper with a short discussion.

2. A DECOMPOSITION ALGORITHM

In [14], Meyer has discussed the classical Rudin-Osher-Fatemi model [15]. He has introduced a new model to split a given image f into a sum $u + v$ of a bounded variation component and a component containing the oscillating part of the image. The u component can be viewed as a sketch of the original image f. This model has first been successfully implemented by Vese and Osher [10]. A different approach has been proposed in [11, 12]. We will use this one, where the decomposition is computed by minimizing a convex functional which depends on the two variables u and v, alternatively in each variable. Each minimization is based on a projection algorithm to minimize the total variation [16]. See also [17, 18] for other interesting approaches.

2.1. Modelling

Let Ω be a bounded open set of $\mathbb{R}^2$ with Lipschitz boundary. The space used to model the geometrical component u of an image f is the space BV of functions with bounded variation. We recall here its definition [16]:
Definition: $BV(\Omega)$ is the subspace of functions $u \in L^1(\Omega)$ such that the following quantity is finite:

$$J(u) = \sup \left\{ \int_\Omega u(x) \text{div}\,(\xi(x)) dx, \quad \xi \in C_c^1(\Omega; \mathbb{R}^2), \|\xi\|_{L^\infty(\Omega)} \leq 1 \right\} \quad (1)$$

$BV(\Omega)$ endowed with the norm $\|u\|_{BV(\Omega)} = \|u\|_{L^1(\Omega)} + J(u)$ is a Banach space. If $u \in BV(\Omega)$, the distributional derivative Du is a bounded Radon measure and (1) corresponds to the total variation $|Du|(\Omega)$.
In [14], Meyer has proposed a new decomposition model:

$$\inf_{(u,v) \in BV(\Omega) \times G(\Omega) / f = u+v} (J(u) + \alpha \|v\|_G) \quad (2)$$

The Banach space $G(\Omega)$ contains signals with large oscillations, and thus in particular textures and noise. The G-norm replaces the classical L^2 norm of the Rudin-Osher-Fatemi model [15]. We give here the definition of $G(\Omega)$:
Definition: $G(\Omega)$ is the Banach space composed of the distributions f which can be written

$$f = \partial_1 g_1 + \partial_2 g_2 = \text{div}\,(g) \quad (3)$$

with g_1 and g_2 in $L^\infty(\Omega)$. On G, the following norm is defined:

$$\|v\|_G = \inf \left\{ \|g\|_{L^\infty(\Omega)} = \operatorname*{ess\,sup}_{x \in \Omega} |g(x)| \ / v = \text{div}\,(g), \quad g = (g_1, g_2),\ g_1 \in L^\infty(\Omega), g_2 \in L^\infty(\Omega), \quad |g(x)| = \sqrt{|g_1|^2 + |g_2|^2}(x) \right\} \quad (4)$$

A function belonging to G may have large oscillations and nevertheless have a small norm [14, 18].

2.2. Functional

In [11, 12], the authors have introduced the following functional:

$$\inf_{(u,v) \in BV(\Omega) G_\mu(\Omega)} \left(J(u) + \frac{1}{2\lambda} \|f - u - v\|^2_{L^2(\Omega)} \right) \quad (5)$$

where

$$G_\mu(\Omega) = \{ v \in G(\Omega) / \|v\|_G \leq \mu \} \quad (6)$$

The parameter λ controls the L^2-norm of the residual $f - u - v$. The smaller it is, the smaller the L^2-norm of the residual gets. And μ controls the G-norm of the oscillating part v. It is shown in [11, 12] that solving (5) is a way to solve (2).

Figure 1: *Barbara image*

The minimum of (5) is computed by minimizing alternatively in each variable u and v. Each minimization is based on a projection algorithm to minimize the total variation [16].
We denote by P_K the orthogonal projection on a set K. When $K = G_\mu$ for some $\mu > 0$, this projection is computed thanks to Chambolle's algorithm [16].
Algorithm:

1. Initialization:
$$u_0 = v_0 = 0 \quad (7)$$
2. Iterations:
$$v_{n+1} = P_{G_\mu}(f - u_n) \quad (8)$$
$$u_{n+1} = f - v_{n+1} - P_{G_\lambda}(f - v_{n+1}) \quad (9)$$
3. Stopping test: we stop if
$$\max(|u_{n+1} - u_n|, |v_{n+1} - v_n|) \leq \epsilon \quad (10)$$

2.3. Numerical experiments

In the results that we present in this subsection, we have decided to add the small residual $f - u - v$ to the geometrical component. This way, we have an exact decomposition, which is a good point since we intend to carry out approximation on this decomposition. Figures 1 and 2 are the images which we want to decompose. The numerical results are displayed on Figures 3, 4, 5 and 6.

Figure 2: *Lighthouse image*

Figure 3: BV *component* u *of the Barbara image (*$\lambda = 0.1$ *and* $\mu = 60$*).*

3. NONLINEAR MULTISCALE REPRESENTATIONS FOR GEOMETRICAL IMAGES

While standard 2-d wavelets provide sparse representations of smooth textured images, they are not able to exploit the fact that the discontinuities (edges) delineating different textured regions lie along smooth contours, leading to poor algorithmic performance results. This has motivated new directions of research towards compact representations of geometry : curvelets [2], contourlets [3] and bandlets [4]. Edge adapted (EA) multiscale representations introduced and studied in [5, 8] are another possible track for such improvements. This transform has as guideline the discrete 1-d framework of Ami Harten [19].

3.1. Harten's framework

The ideas of A. Harten can be described as follows: we start from a finite set $v^J = (v_k^J)$ of discrete data at the resolution level J. For all j, we define a decimation operator D_j^{j-1}, which extracts from (v_k^j) the discrete data (v_k^{j-1}) at the next coarser level, and a prediction operator P_{j-1}^j, which yields an approximation $(\hat{v}_k^j)$ of (v_k^j) from (v_k^{j-1}). The decimation is always a linear operator, and the prediction is allowed to be a nonlinear operator, but they satisfy the following consistency condition $D_j^{j-1} P_{j-1}^j = I$. Consequently, we represent v^j in terms of (v^{j-1}, e^{j-1}), where e^{j-1} is the prediction error which belongs to the null space of D_j^{j-1} (due to the consistency relation). We represent the error e^j in terms of a basis of the null space of D_j^{j-1}, resulting in the detail vector d^{j-1}. Therefore we can represent v^j by (v^{j-1}, d^{j-1}). By iterating this procedure from the finest level J to the coarsest level $j = 0$ we obtain the multiscale representation of v^J into $(v^0, d^0, ..., d^{J-1})$.

3.2. Edge Adapted multiresolution representations

3.2.1. 1-d formalism

For the sake of clarity, we consider here the 1-d case (for the 2-d case, we refer the reader to [5, 7, 8]). We consider hierarchical discretizations by cell-averages $v_k^j := 2^j \int_{c_k^j} v(x)dx$, where $c_k^j := [k2^{-j}, (k+1)2^{-j})$. This choice fixes the decimation as $v_k^{j-1} := \frac{1}{2}(v_{2k}^j + v_{2k+1}^j)$. Using $e_{2k}^{j-1} + e_{2k+1}^{j-1} = 0$, we define the details by $d_k^{j-1} = e_{2k}^j$.

We now want to define a good prediction operator which makes the approximation error and then the detail coefficents as small as possible, resulting in a sparse representation. The simplest choice for such an operator is $\hat{v}_{2k}^j = \hat{v}_{2k+1}^j = v_k^{j-1}$, which corresponds to the decomposition in the Haar system with a low order of accuracy. The order of approximation can be raised by using a higher order polynomial reconstruction, by defining p_k^{j-1} as the unique quadratic polynomial which fits the averages $(v_{k-1}^{j-1}, v_k^{j-1}, v_{k+1}^{j-1})$, and by defining $\hat{v}_{2k}^j$ and $\hat{v}_{2k+1}^j$ as the averages of p_k^{j-1} on the corresponding intervals. The resulting multiscale transform is equivalent to the biorthogonal wavelet transform (BW), raising the approximation order in smooth regions and also generating oscillations

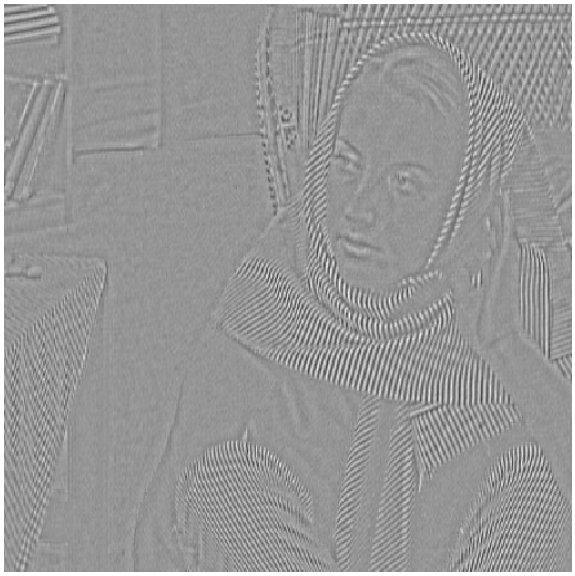

Figure 4: *Oscillatory component v of the Barbara image ($\lambda = 0.1$ and $\mu = 60$).*

Figure 5: *BV component u of the lighthouse image ($\lambda = 0.1$ and $\mu = 12$).*

near singularities.

ENO mechanism: we can improve the method by using a nonlinear prediction operator, such as *essentially non-oscillatory* (ENO) reconstruction, as proposed in [19]. The goal of such an operator is to improve the approximation order near the singularities. The ENO reconstruction chooses among the polynomials $(p_{k-1}^{j-1}, p_k^{j-1}, p_{k+1}^{j-1})$ the least oscillatory one with respect to some numerical criterion based only on the values at the coarser level.

Subcell resolution technique: we can go further with these ideas by using the subcell resolution technique in the cells containing singularities. These cells are detected as those for which the supports of the adjacent polynomials (selected by the ENO mechanism) do not intersect (see figure 7).

For such cells, we then use a piecewise polynomial reconstruction $p_{k-2}^{j-1}\mathbf{1}_{]-\infty,y]} + p_{k+2}^{j-1}\mathbf{1}_{[y,\infty[}$, where y is obtained by consistency with the average v_k^{j-1}.

Example: in Figure 8 we show the reconstruction of a piecewise smooth function from a resolution level of 3. This illustrates the accuracy of our nonlinear reconstruction method (ENO-SR). BW prediction is accurate for smooth functions and exact for poynomial functions, while ENO-SR prediction is accurate for piecewise smooth functions and exact for piecewise polynomial functions.

3.2.2. Edge Adapted prediction for images

All the ideas developed in the 1-d case can be generalised to the 2-d case (with some technical tricks).

For more details on EA prediction we refer the reader to [5], [6] and [7] where this procedure has been introduced and where some properties have been investigated, namely the exactness of the prediction operator with respect to simplified model and also the approximation order.

4. A NEW NONLINEAR APPROXIMATION ALGORITHM

4.1. Presentation

The algorithm presented in Section 3 (EA) is an efficient approximation algorithm for geometrical images. Its performance comes from the fact that it takes into account the geometry of the image. Such an algorithm is thus particularily well suited for the approximation of the geometrical component of an image.

The idea of our algorithm (UVEA) is the following. We first decompose our original image f into two components u and v with the algorithm presented in Section 2 , u being the geometrical component, and v the oscillatory part. We then use the approximation algorithm of Section 3 (EA) on u, and a classical approximation algorithm on v. For v, we have decided to use the 7-9 biorthogonal wavelets (BW) [1].

4.2. Numerical results and comments

Figure 1 is the Barbara image which we want to approximate. When testing our algorithm, we have chosen to use

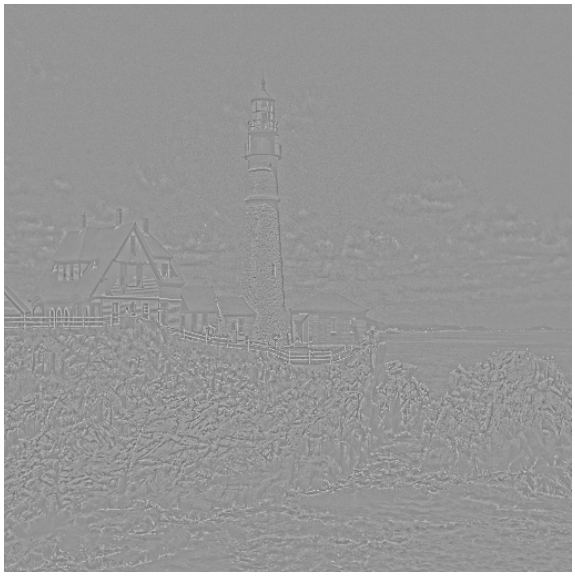

Figure 6: *Oscillatory component v of the lightouse image ($\lambda = 0.1$ and $\mu = 12$).*

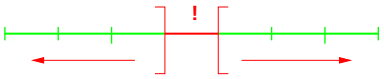

Figure 7: *Singular cell*

images such as this one: images containing both geometrical and texture information. Figure 9 is the result we get with our algorithm. We have kept 7% of the coefficients of the geometrical part and 13% for the textured part.
Figure 10 is the result we get with the EA algorithm. We have kept 20% of the coefficients. Since it has been developed for geometrical image, it performs not very well with images containing textures. Figure 11 is the result we get with the standard BW algorithm (we have also kept 20% of the coefficients so that we can compare the results).
Table 1 shows the L^2-error. The best L^2-error is perfomed by our algorithm. Moreover, the geometrical information of the image is much more preserved with our algorithm than with BW: this can be checked on the leg of the table for instance (see also Figure 12 which is a zoom of Barbara's shoulder). And some textures which disappear with the BW algorithm are preserved with our algorithm (see

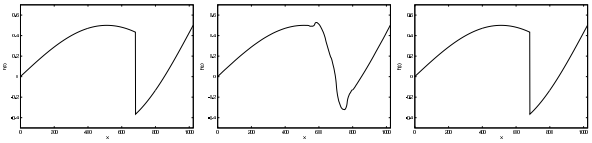

Figure 8: *(a) Original function, (b) BW and (c) ENO-SR*

Figure 9: *Compressed image with our method (UVEA) (7% of the coefficients for the u component and 13% for the v component)*

Figure 13 which is a zoom of Barbara's knee). Therefore, our algorithm gives a better result than the BW algorithm.

We have conducted experiments on several images, and this has confirmed these results. For instance, Figure 14 shows the result we get with our algorithm with the lighthouse image of Figure 2. We have kept 10% of the coefficients of both the geometrical part and the textured part. And Figure 15 is the result we get with the BW algorithm (with 20% of the coefficients). The same conclusions hold for the lighthouse image as for the Barbara image (see Table 2).

Table 1: L^2-errors (Barbara image)

Algorithm	UVEA	EA	BW
L^2-error	14.97	19.94	15.75
PSNR	24.79	22.13	24.23

Table 2: L^2-errors (lighthouse image)

Algorithm	UVEA	BW
L^2-error	9.14	9.96
PSNR	28.88	28.19

Figure 10: *Compressed image with EA (*20% *of the coefficients)*

Figure 11: *Compressed image with biorthogonal wavelets (BW) (*20% *of the coefficients)*

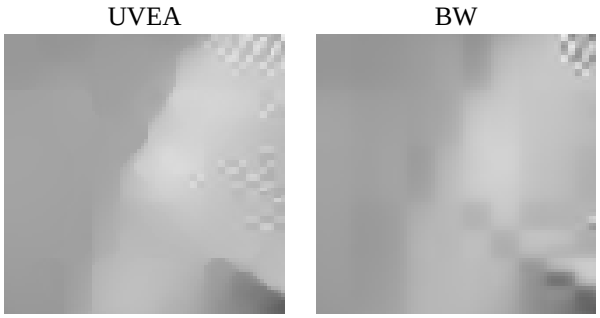

Figure 12: *Zoom on Barbara's shoulder*

5. CONCLUSION AND FUTURE PROSPECTS

We have presented a new nonlinear approximation algorithm for images containing both structure and texture information. We first split the image to approximate into two components, one containing the structures, and another one the textures. We then carry out the approximation of these two components with adapted algorithms: the EA algorithm of [5] for the geometrical part, and the 7-9 biorthogonal wavelets for the texture part. This procedure gives us a powerful nonlinear approximation algorithm (it indeed leads to a compact representation of the image).

In our numerical tests, it outperforms the standard biorthogonal wavelets (BW) approximation algorithm with respect to both the L^2-norm and the visual aspect of the image: the edges are sharper, and more textures are preserved. This is therefore a very promising way to improve compression rates in image processing.

We now plan to study the best strategy to approximate the geometrical component and the oscillating one. Up to now, we have chosen arbitrarily the number of coefficients for each component. We may improve our compression results with a more subtle choice. We also plan to improve the prediction operator of the EA algorithm, by taking into account that it only deals here with pure geometrical images. We intend to compare the EA algorithm with other nonlinear approximation algorithms for geometrical images [2, 3, 4]. A more detailed version of this work can be found in [20].

6. REFERENCES

[1] S.G. Mallat, *A Wavelet Tour of Signal Processing*, Academic Press, 1998.

[2] E. Candès and D. Donoho, "A surprisingly effective nonadaptive representation for objects with edges," November 1999, Curves and Surfaces, L. L. Schumaker et al. (eds), Vanderbilt University Press, Nashville, TN.

[3] M. Do and M. Vetterli, "The finite ridgelet transform for image representation.," November 2001, Technical Report DSC/2001/019, Communication Systems Department, EPFL (Switzerland).

[4] E. Le Pennec, "Bandelettes et représentations géométriques des images," December 2002, Ph. D. Thesis, Ecole Polytecnique, Paris.

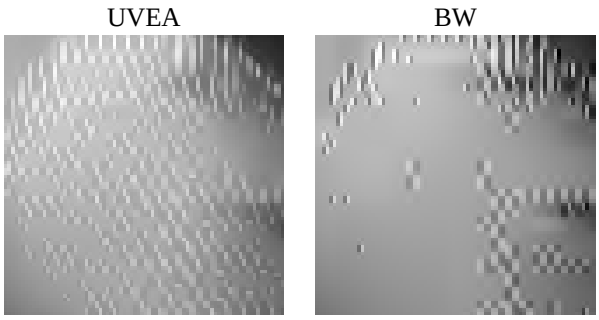

Figure 13: *Zoom on Barbara's knee*

Figure 14: *Compressed image with our algorithm (*10% *of the coefficients for both the* u *and the* v *component)*

[5] B. Matei, "Methodes multi-résolution non-linéaires. applications au traitement d'image," November 2002, Ph. D. Thesis, Université Pierre et Marie Curie, Paris.

[6] A. Cohen and B. Matei, "Nonlinear subdivisions schemes: applications to image processing," July 2002, Tutorial on multiresolution in geometric modelling,A.Iske, E.Quack and M.Floater eds., Springer.

[7] A. Cohen and B. Matei, "Compact representations of images by edge adapted multiscale transforms," September 2001, IEEE ICIP Conference Thessaloniki.

[8] F. Arandiga, A. Cohen, M. Doblas, R. Donat, and B. Matei, "Sparse representations of images by edge adapted nonlinear multiscale transforms," September 2003, IEEE ICIP Conference Barcelona.

Figure 15: *Compressed image with BW (*20% *of the coefficients)*

[9] H.J.A.M. Heijmans, B. Pesquet-Popescu, and G. Pellia, "Building nonredundant adaptive wavelets by update lifting," May 2004, Report PNA-R0212, CWI.

[10] L.A. Vese and S.J. Osher, "Modeling textures with total variation minimization and oscillating patterns in image processing," *Journal of Scientific Computing*, vol. 19, pp. 553–572, 2003.

[11] J.F. Aujol, G. Aubert, L. Blanc-Féraud, and A. Chambolle, "Decomposing an image: Application to textured images and SAR images," 2003, INRIA Research Report 4704, to appear in JMIV, http://www.inria.fr/rrrt/rr-4704.html.

[12] J.F. Aujol, G. Aubert, L. Blanc-Féraud, and A. Chambolle, "Decomposing an image: Application to SAR images," in *Scale-Space '03*, 2003, vol. 1682 of *Lecture Notes in Computer Science*.

[13] M. Bertalmio, L. Vese, G. Sapiro, and S. Osher, "Simultaneous structure and texture image inpainting," *IEEE Transactions on Image Processing*, vol. 12, no. 8, pp. 882–889, 2003.

[14] Yves Meyer, "Oscillating patterns in image processing and in some nonlinear evolution equations," March 2001, The Fifteenth Dean Jacquelines B. Lewis Memorial Lectures.

[15] L. Rudin, S. Osher, and E. Fatemi, "Nonlinear total variation based noise removal algorithms," *Physica D*, vol. 60, pp. 259–268, 1992.

[16] A. Chambolle, “An algorithm for total variation minimization and applications,” *JMIV*, vol. 20, pp. 89–97, 2004.

[17] S.J. Osher, A. Sole, and L.A. Vese, “Image decomposition and restoration using total variation minimization and the H^{-1} norm,” *Multiscale Modeling and Simulation: A SIAM Interdisciplinary Journal*, vol. 1, no. 3, pp. 349–370, 2003.

[18] J.F. Aujol and A. Chambolle, “Dual norms and image decomposition models,” 2004, INRIA Research Report 5130, http://www.inria.fr/rrrt/rr-5130.html, to appear in IJCV.

[19] A. Harten, “Discrete multiresolution analysis and generalized wavelets,” December 1993, Journal of Applied Numerical Mathematics,12:153-193.

[20] J.F. Aujol and B. Matei, “Structure and texture compression,” 2004, INRIA Research Report 5076, http://www.inria.fr/rrrt/rr-5076.html.